Journal of Renewable
Energy and Environment

Research Article

Journal Homepage: www.jree.ir

Numerical Investigation of the Effect of Gas Diffusion Layer with Semicircular prominences on Polymer Exchange Membrane Fuel Cell Performance and Species Distribution

N. Ahmadi*, S. Rezazadeh, A. Dadvand, I. Mirzaee

Department of Mechanical Engineering, Urmia University of Technology, Urmia, Iran

PAPER INFO

Paper history:
Received 24 April 2015
Accepted in revised form 11 October 2015

Keywords:
Polymer Exchange Membrane
Gas Diffusion Layer
current density
prominence
Finite volume

ABSTRACT

A three-dimensional computational fluid dynamics model of a proton exchange membrane fuel cell (PEMFC) with both gas distribution flow channels and Membrane Electrode Assembly (MEA) is developed. A set of conservation equation is numerically solved by developing a CFD code based on the finite volume technique and SIMPLE algorithm. In this research, some parameters like oxygen consumption, water production, velocity distribution, liquid water activity and the fuel cell performance for conventional cases (base Cases) are presented and compared to those in cases with semicircular prominences. The numerical simulations indicated that prominent gas diffusion layer (GDL) could improve the transport of the species through the porous layers and this leads to increment in fuel cell performance. Hence, prominent gas diffusion layers would result in higher current density. Finally the numerical results for the base Cases were compared with the experimental data, which represented reasonable agreement.

1. INTRODUCTION

Proton exchange membrane fuel cell (PEMFC) with very thin polymer membrane as electrolyte is considered as a promising candidate for future power sources, especially for transportation applications and residential power. This type of fuel cell has many significant advantages like high-efficiency, clean, quiet and low-temperature operation, capability of quick start-up, no liquid electrolyte and simple cell design. However, its performances and costs should be more optimized before entering the system in competition with traditional combustion power plants. Shimpalee et al. [1] studied the effect of channel path length on PEMFC flow-field design. Yima et al. [2] investigated the operation of PEMFC stack under low humidifying condition. The effect of angle and height of trapezoid baffle on the PEMFC's net power output was studied by Perng et al. [3].

In recent years, research and development in fuel cells and fuel cell systems have been accelerated. However, fuel cell systems are still cost a fortune to become viable commercial products. In a fuel cell, fuel (e.g., hydrogen gas) and an oxidant (e.g., oxygen gas from the air) are used to generate electricity, while heat and water are typical products of the fuel cell operation. A fuel cell generally operates based on the following principle: as hydrogen gas flows into the fuel cell on the anode side, a platinum catalyst facilitates oxidation of hydrogen gas, which produces protons (hydrogen ions) and electrons. Hydrogen ions diffuse through a membrane (the center of the fuel cell separating the anode and the cathode) and combine with oxygen and electrons on the cathode side via a platinum catalyst in order to produce water. The electrons, which cannot pass through the membrane flow from anode to cathode through an external electrical circuit containing a motor or other electric system.

Both anode and cathode (i.e.,the electrodes) are porous and t made of an electrically conductive material(e.g., carbon). The electrode faces are in contact with the membrane containing carbon, polymer electrolyte and a platinum-based catalyst. The oxidation and reduction fuel-cell half reactions take place in anode and cathode active layers, respectively. The polymer electrolyte membrane (PEM) electrodes are of gas-diffusion type

*Corresponding Author's Email: nima.ahmadi.eng@gmail.com (N. Ahmadi)

and generally designed to have maximum surface area per unit material volume (the specific surface area). In this way, gas-diffusion layer can be available for the reactions in order to minimize the transport resistance of hydrogen and oxygen in active layers.

In the past decade, extensive researches have been conducted to develop realistic simulation models. Researchers all over the world are focusing on optimizing the fuel cell system to be cost competitive with currently available energy conversion devices. For example Grujicic et al. [4] presented the study of the PEM fuel cells optimization.

Many studies have examined various aspects of PEMFC performances as a function of operating conditions. Xing et al. [5] optimized the assembly clamping pressure effect on the performance of PEMFCs. Chang et al. [6] developed the research, which indicated the effect of clamping pressure on the PEM fuel cell performance [6].Kyle [7] presented different reconstruction algorithms to determine the effective transport properties in a PEMFC catalyst layer. Amphlett et al. [8] modeled the performance of the Ballard Mark IV solid polymer electrolyte fuel cell(SPEFC). Guangli et al. [9] offered a 3-D model of two phases PEMFC. Nath et al. [10] introduced an organic compound methyl methane sulfonate applicable in fabrication of polystyrene based PEM using plasma polymerization process. Jinlong et al. [11] investigated the effect of strain on corrosion resistance of 316L stainless steel as bipolar plates in PEMFC environment. Uribe et al. [12] studied the effect of ammonia as fuel impurity on PEMFC [12].Ticianelli et al. [13] localized platinum in low catalyst loading electrodes to achieve high power densities in SPEFCs. One of the important tools in optimization study of fuel cell performance is computational modeling, which can give insight understanding of the fundamental phenomena replacing the fuel cell system. Yao et al. [14] presented a sophisticated review of the mathematical models for hydrogen and direct methanol polymer electrolyte membrane fuel cells. A two-dimensional two phase transient model of PEMFC was given by Natarajan et al. [15].

A great number of researches have been conducted to improve the performance of the PEMFC, so that it can achieve a significant market penetration. The performance of PEMFCs is influenced by many parameters such as operating temperature, pressure, humidification of the gas streams and geometrical and Among these, the geometrical plays a major role. For instance, the performance of a fuel cell with smaller shoulder widths will be better than of those with larger ones. Ahmadi et al. [16] studied the effect of inlet gases humidity on PEMFC performance [16]. Validation and parametric study of PEMFC were investigated by Lum et al. [17].Effects of channel geometrical configuration and shoulder width on PEMFC performance were investigated through a good work presented by Ahmed et al. [18].

The effect of gas channel geometry on the performance of PEMFCs was studied by many researchers. The effect of step-like gas channel on the efficiency of the PEMFC is studied by Ahmadi et al. [19] and in et al.[20] investigated the PEMFC performance through the consideration of different cell potentials [20].also in et al. [21] Ahmadi studied the effect of parallelogram gas channel and shoulder geometry on the fuel cell performance. Ahmadi et al. [22] also conducted the numerical study to deliberate the effect of prominent gas diffusion layers (GDLs) on the PEMFC performance. Results for the cubical prominences showed that locating the prominences on the GDLs led to significant increment in the PEMFC performance. Ahmed and Sung [23] performed simulations of PEMFCs with a new design for the channel shoulder geometry [23].

In the present work, a three-dimensional, single phase, non-isothermal and parallel flow model of a PEMFC with conventional membrane electrode assembly (MEA)and semicircular prominent GDLs are simulated numerically. The numerical results reveal that the prominent GDLs lead to significant increase in cell current density. The available experimental data are used in order to validate the results of polarization curve for conventional model. In this model, the major transport phenomena of PEMFC is investigated carefully.

2. MATHEMATICAL MODEL

Figures 1. and 2. show respectively the front and side views of single cell of a PEMFC (base model). It is made of two porous electrodes, a polymer electrolyte membrane, two catalyst layers and two gas distributor plates. The membrane has been located between the gas channels.

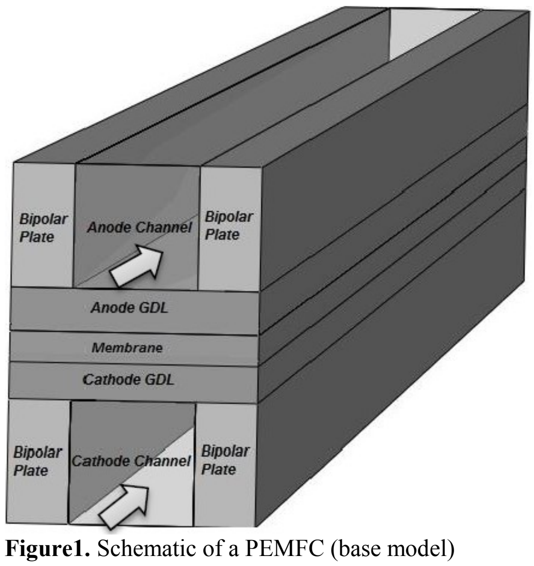

Figure1. Schematic of a PEMFC (base model)

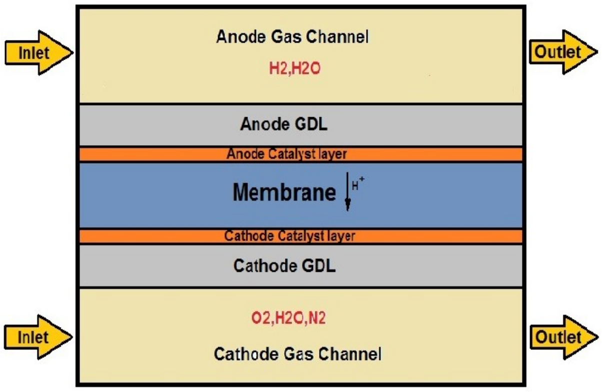

Figure 2. Side view schematic of the base model

2.1. Model assumption In the present work, the following assumptions have been made: (i) all gases are assumed to be ideal gas mixture, GDLs and catalyst layers are homogeneous porous;(ii) the fuel cell is assumed non-isothermal; (iii) the flow is steady state, incompressible and laminar;(iv) since the pressure gradients and velocities are small and the volume of liquid water in the domain is negligible, the flow field is considered single phase.

2.2. Governing equation The governing equations employed in the present work consist of the continuity, momentum, species and charge equations, which can be written as:

$$(\nabla . \rho \mathbf{u}) = 0 \tag{1}$$

$$\frac{1}{(\varepsilon^{eff})^2} \nabla . (\rho \mathbf{u} \mathbf{u}) = -\nabla P + \nabla . (\mu \nabla \mathbf{u}) + S_u \tag{2}$$

$$\nabla . (\mathbf{u} C_K) = \nabla . (D_K^{eff} \nabla C_K) + S_K \tag{3}$$

$$\nabla . (\kappa_e^{eff} \nabla \Phi_e) + S_\Phi = 0 \tag{4}$$

In Eq. (1) ρ is the density of gas mixture. According to model assumptions, the mass source and sink term were neglected. ε is the effective porosity inside porous media. μ is the viscosity of the gas mixture in the momentum equation (2). The momentum source term Su is used to describe the Darcy's drag for flow through porous gas diffusion and catalyst layers [3]:

$$S_u = -\frac{\mu}{K} \mathbf{u} \tag{5}$$

Where, K is the gas permeability inside porous media. D_K^{eff} in the species equation (3) is the effective diffusion coefficient of species K (e.g., hydrogen, oxygen, nitrogen and water vapor). It is defined by the Bruggeman correlation [13] to describe the effects of porosity on the porous gas diffusion and catalyst layers:

$$D_K^{eff} = (\varepsilon^{eff})^{1.5} D_K \tag{6}$$

Additionally, the diffusion coefficient is a function of temperature and pressure presented by next equation [14]:

$$D_K = D_K^{\circ} \left(\frac{T}{T_{\circ}}\right)^{\frac{3}{2}} \left(\frac{P_{\circ}}{P}\right) \tag{7}$$

The transport properties of the species are given in Table 1.

TABLE 1. Transport properties of the species[14]

Property	Value (m^2/s)
H_2 Diffusivity in the gas channel, $D^{\circ}_{H_2}$	1.10×10^{-04}
O_2 Diffusivity in the gas channel, $D^{\circ}_{O_2}$	3.20×10^{-05}
H_2O Diffusivity in the gas channel, $D^{\circ}_{H_2O}$	7.35×10^{-05}
H_2 Diffusivity in the membrane, $D^{mem}_{H_2O}$	2.59×10^{-10}
O_2 Diffusivity in the membrane, $D^{mem}_{O_2}$	1.22×10^{-10}

The charge conservation equation is shown as Eq. (4) where κ_e denotes the ionic conductivity in the ion metric phase defined by Springer et al. [15] as

$$\kappa_e = \exp\left[1268\left(\frac{1}{303} - \frac{1}{T}\right)\right] \times (0.005139\ \lambda - 0.00326) \tag{8}$$

In Eq. (8), λ denotes the number of water molecules per sulfonate group inside the membrane defined according to experimental data as follows [16]:

$$\lambda = 0.3 + 0.6a[1 - \tanh(a - 0.5)] + 3.9\sqrt{a}\left[1 + \tanh\left(\frac{a - 0.89}{0.23}\right)\right] \tag{9}$$

The water content λ can be assumed function of water activity *a* defined as:

$$a = \frac{C_w R T}{P_w^{sat}} \tag{10}$$

The proton conductivity in the catalyst layers is given by the Bruggeman correlation [13]:

$$\kappa_e^{eff} = \varepsilon_m^{1.5} \kappa_e \tag{11}$$

In the recent equation, ε_m is the volume fraction of the membrane-phase in the catalyst layer. The source and sink terms in Esq. (3) and (4) are presented in Table 2. The local current density in the membrane can be calculated by:

$$I = -\kappa_e \nabla \Phi_e \tag{12}$$

Then the average current density is calculated as follows:

$$I_{ave} = \frac{1}{A} \int_{A_{mem}} I\, dA \tag{13}$$

Where, *A* is the active area over the MEA.

TABLE 2. Source/sink terms in the momentum, species and charge conservation equations for individual regions

Zone	Momentum	species	charge
Flow channels	$S_u = 0$	$S_K = 0$	$S_\Phi = 0$
Bipolar plates	$S_u = -\frac{\mu}{K}\mathbf{u}$	$S_K = 0$	$S_\Phi = 0$
GDLs	$S_u = -\frac{\mu}{K}\mathbf{u}$	$S_K = 0$	$S_\Phi = 0$
Catalyst layers	$S_u = 0$	$S_K = -\nabla.\left(\frac{n_d}{F}I\right) - \frac{S_K j}{nF}$	$S_\Phi = j$
Membrane	$S_u = 0$	$S_K = -\nabla.\left(\frac{n_d}{F}I\right)$	$S_\Phi = 0$

2.3. Water transport

Due to the properties of polymer electrolyte membrane and the molecular diffusion, water molecules in PEMFC are transported via electro-osmotic drag. H^+ protons transport water molecules through the polymer electrolyte membrane. This transport phenomenon is called electro-osmotic drag. In addition to the molecular diffusion and electro-osmotic drag, water vapor is also produced in the catalyst layers due to the oxygen reduction reaction.

The water transport through the polymer electrolyte membrane is defined by:

$$\nabla.\left(D_{H_2O}^{mem}\nabla C_{H_2O}^{mem}\right) - \nabla.\left(\frac{n_d}{F}i\right) = 0 \quad (14)$$

Where nd and $D_{H_2O}^{mem}$ denote the water drag coefficient from anode to cathode and the diffusion coefficient of water in the membrane phase, respectively. The number of water molecules, transported by each hydrogen proton H^+, is called the water drag coefficient. It can be determined from the following equation [24-25]:

$$n_d = \begin{cases} 1 & \lambda < 9 \\ 0.117\lambda - 0.0544 & \lambda \geq 9 \end{cases} \quad (15)$$

The diffusion coefficient of water in the polymer membrane depends on the water content of the membrane. It was developed by the following fits of the experimental expression [26]:

$$D_w^{mem} = \begin{cases} 3.1\times10^{-7}\lambda\left(e^{0.28\lambda}-1\right)e^{\left(\frac{-2346}{T}\right)} & 0 < \lambda \leq 3 \\ 4.17\times10^{-8}\left(1+161e^{-\lambda}\right)e^{\left(\frac{-2346}{T}\right)} & Otherwise \end{cases} \quad (16)$$

Therefore, the terms are function of the transfer current through the solid conductive materials and the membrane. The transfer currents or source terms are non-zero only inside the catalyst layers. The transfer currents at the anode and cathode side are described by Tafel equations [27]:

$$R_{an} = j_{an}^{ref}\left(\frac{[H_2]}{[H_2]_{ref}}\right)^{\gamma_{an}}\left(e^{\alpha_{am}F\eta_{an}/RT} - e^{-\alpha_{cat}F\eta_{an}/RT}\right) \quad (17)$$

$$R_{cat} = j_{an}^{ref}\left(\frac{[O_2]}{[O_2]_{ref}}\right)^{\gamma_{cat}}\left(-e^{\alpha_{am}F\eta_{cat}/RT} + e^{-\alpha_{cat}F\eta_{cat}/RT}\right) \quad (18)$$

According to the Tafel equations, the current densities in the anode and cathode catalysts can be expressed by the exchange current density, reactant concentration, temperature and over-potentials. The surface over-potential is defined as the difference between proton potential and electron potential.

$$\eta_{an} = \varphi_{sol} - \varphi_{mem} \quad (19)$$

$$\eta_{cat} = \varphi_{sol} - \varphi_{mem} - V_{oc} \quad (20)$$

The open circuit potential at the anode is assumed to be zero, while that at the cathode is a function of temperature:

$$V_{oc} = 0.0025T + 0.2329 \quad (21)$$

The protonic conductivity of membrane σm is a function of water content, which has been correlated by Springer et al. [27]:

$$\sigma_m = (0.005139\lambda - 0.00326)\exp\left[1268\left(\frac{1}{303} - \frac{1}{T}\right)\right] \quad (22)$$

The energy equation is given by:

$$\nabla.(\rho\mathbf{u}T) = \nabla.(\lambda_{eff}\nabla T) + s_T \quad (23)$$

Where λ_{eff} is the effective thermal conductivity and S_T is the source term, which is defined by the following equation [16]:

$$S_T = I^2R_{ohm} + h_{reaction} + \eta_a i_a + \eta_c i_c \quad (24)$$

In Eq. (24) R_{ohm} is the ohmic resistance of the membrane, $h_{reaction}$ denotes the heat generated through the chemical reactions, and η_a and η_c are the anode and cathode over-potentials, which are calculated as follows:

$$R_{ohm} = \frac{t_m}{\sigma_m} \quad (25)$$

$$\eta_a = \frac{RT}{\alpha_a F}\ln\left[\frac{IP}{j_{0_a}P_{0_{H_2}}}\right] \quad (26)$$

$$\eta_c = \frac{RT}{\alpha_c F}\ln\left[\frac{IP}{j_{0_c}P_{0_{O_2}}}\right] \quad (27)$$

where, t_m is the membrane thickness, αa and αc are the anode and cathode transfer coefficients, $P_{0_{H_2}}$, $P_{0_{O_2}}$ are the partial pressure of hydrogen and oxygen, respectively and finally j_0 is the reference exchange current density. The fuel and oxidant fuel rate $\boldsymbol{u}$ is given by the following relations:

$$\boldsymbol{u}_{in,a} = \frac{\xi_a I_{ref} A_{mem}}{2C_{H_2,in}FA_{ch}} \quad (28)$$

$$u_{in,c} = \frac{\xi_c I_{ref} A_{mem}}{4 C_{O_2,in} F A_{ch}}$$

Where, I_{ref} and ξ are the reference current density and stoichiometric ratio, respectively, ξ is defined as the ratio between the supplied and required amount for the fuel, based on the reference current density. The species concentrations of flow inlets are assigned by the humidification conditions of both the anode and cathode inlets [16].

2.4. Boundary conditions Equations (1) to (4) form the complete set of governing equations in the present mathematical model. Boundary conditions are dispensed at the external boundaries. Constant mass flow rate at the channel inlet and constant pressure condition at the channel outlet are considered. No-flux conditions are considered for mass, momentum, species and potential conservation equations on all boundaries except the inlets and outlets of the anode and cathode flow channels.

3. RESULTS AND DISCUSSIONS

3.1. Model's validation In order to extract the polarization (voltage versus current density) curve, a series of simulations was carried out on the model from low to high operating current densities. The results are illustrated in Figure 3. In addition to substantiate the reliability of the model, the current numerical results associated with the conventional (base) model are compared with the experimental data reported by Wang et al. [28] (see Figure 3.) showing a favorable agreement. The power density curve of the model is also illustrated in Figure 3. According to physical relations, there is a relation between voltage, current density and the power of the fuel cell (i.e., P=V×I). The fuel cell operating condition and geometric parameters are shown in Table3. A fully humidified inlet condition for anode and cathode was used to achieve better performance.

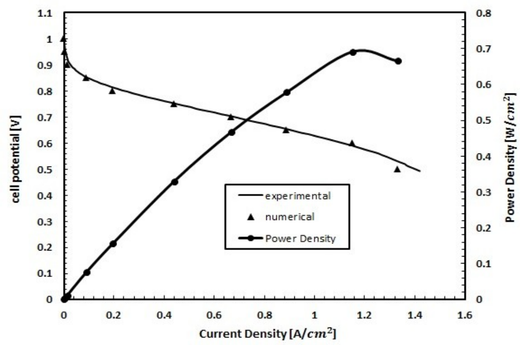

Figure 3. Comparison of polarization curve associated with the current numerical results with the experimental data of [28], and the power density curve at 1.5 (A/m2)

Inconsistency between the simulation results and experimental data can be seen at high current density. This is due to the assumption of the single phase model, i.e., the whole generated water exists in the vapor phase so that the oxygen flux decay due to the presence of liquid water in the catalyst and gas diffusion layers can be neglected. In fact, liquid water fills the pores of the catalyst and gas diffusion layers and consequently increases the mass transfer resistance. Thee dryness of anode is a major factor that reduces the performance of PEMFC sat the high current densities**.**

TABLE 3. Geometrical parameters and operating conditions [18]

Parameter	Value
Gas channel length	7.0×10^{-2} m
Gas channel width and depth	1.0×10^{-3} m
Bipolar plate width	5.0×10^{-4} m
Gas diffusion layer thickness	3.0×10^{-4} m
Catalyst layer thickness	1.29×10^{-5} m
Membrane thickness	1.08×10^{-4} m
Cell temperature	343.15 K
Anode pressure	3 atm
Cathode pressure	3 atm

3.2. Grid independenec study A structured grid is used in the base model. At the catalyst layers where the electrochemical reactions occur, the grid is taken to be finer. Also grid independence test was carried out and finally the optimum number of meshes (174 000cells) was chosen (see Figure 4a). The number of iterations was determined to be 2000 for low current density and 12000 for high current density. An IBM-PC-Pentium 5 (CPU speed is 3.4 GHz) was used to solve the set of equations. The computational time for solving the set of equations was 9hours. Figure 4b. indicates the solution procedure algorithm for numerical simulation.

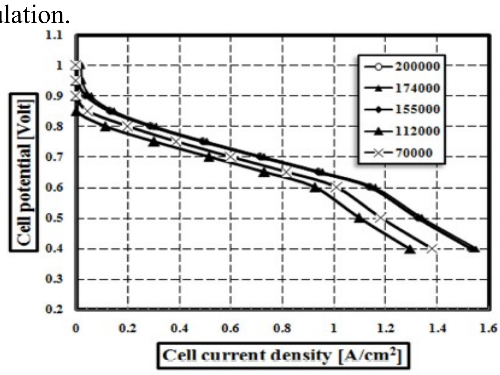

Figure 4a. Grid independence test associated with the polarization curve.

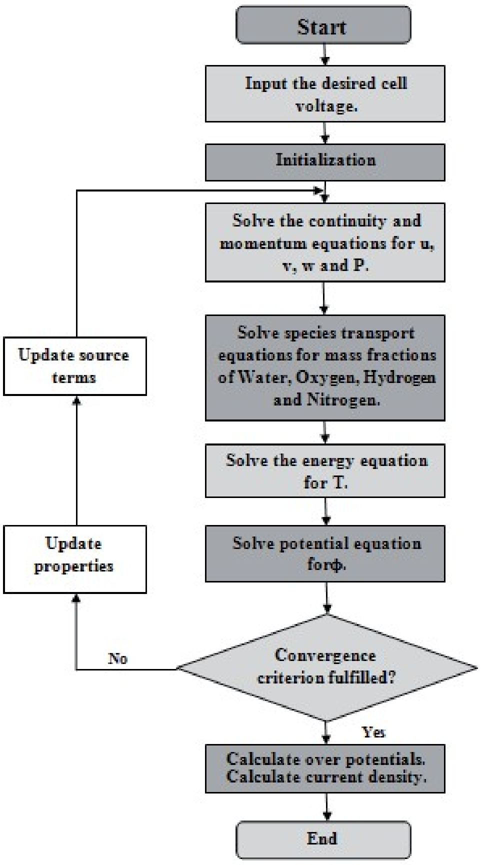

Figure 4b. Solution procedure algorithm

3.3. Numerical models

In the present study a conventional model of PEMFC was numerically modeled and validated against experimental data. Then the effect of semicircular prominences on GDLs was investigated numerically in more details. The numerical result of the case with prominence is compared to that of the conventional (base) model to understand the effect of prominence on the cell performance and its efficiency. The operating conditions of the case with prominence are identical to those of the base model. Figures 5. and 6. illustrate the schematic configuration of the case with semicircular prominences on its GDLs. The geometrical configuration of the prominent case has been presented in Table 4.

Figure 7. compares the polarization and power density curves of two cases. It is clear that, at the same cell voltage, the case with prominences produces more current density than the conventional model.This is because of the increase in the area of diffusion surfaces for the species in the gas channels (the nozzle-like effect). The prominences would reduce the cross sectional area of the channel then lead to an increase in the gas velocity.The nozzle-like effect of GDL prominence decreases the cross sectional area of the reactant gas flow and lead to an increase in the velocity of the reactant gas. This, in turn, enhances the term of convection mass transfer.

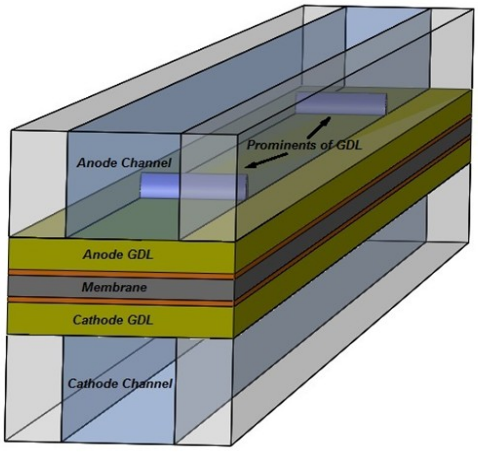

Figure 5. 3-D schematic of a PEMFC(the case with semicircular prominent GDLs).

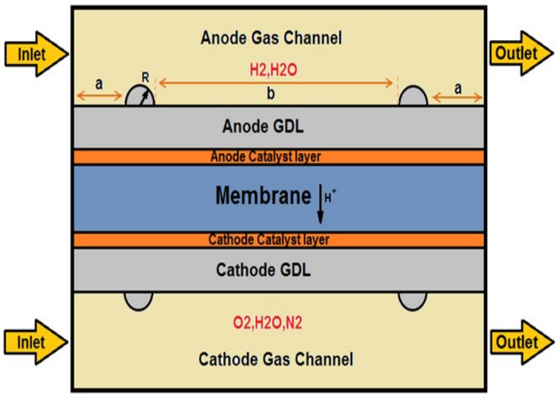

Figure 6. Side view of the case with prominent GDLs.

Also, these prominences increase the GDLs interfaces and the diffusion surface of the reactant. Therefore, the GDLs can supply the reactant to the reaction area more appropriately and uniformly than the conventional model. In the case with prominences, the concentration loss due to mass transfer problems decreases significantly. All these factors lead to enhancing the PEMFC's performance and efficiency.

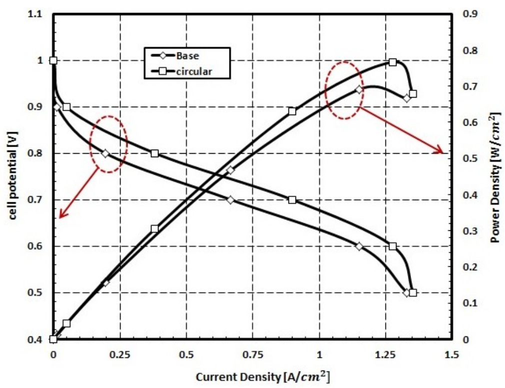

Figure 7. Comparison of the polarization and power density curves associated with two different models.

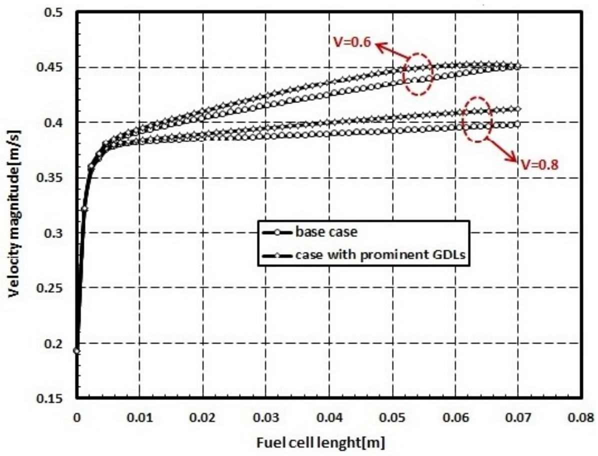

Figure 8. Comparison of the velocity magnitude of the two different models along the cathode gas flow channel (for V=0.6 v, 0.8 v).

TABLE 4. Geometrical configuration of the case with prominences

Symbol	Value
a	15mm
b	40mm
R	0.25mm

Figure 8. indicates the comparison of the velocity magnitude along the cathode gas channel for two different cases. It is clear that the case with semicircular prominences increases the velocity magnitude along the channel significantly due to decrease in flow area in the channel. In addition, the prominences of GDL layers affect the membrane drawing effect positively.

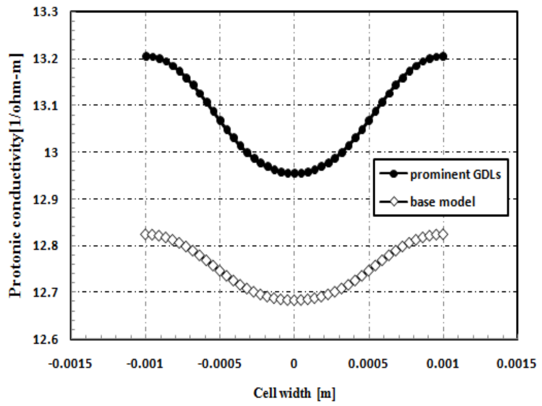

Figure 9. Comparison of the protonic conductivity in the inlet region (z=10 mm)

It is clear from Eq. (22) that, the protonic conductivity of membrane is a function of the membrane water content and temperature. Figures 10. and 11. depict the protonic conductivity for the base model and the model with semicircular prominences respectively in the inlet region and outlet region of the PEMFC attained at the V=0.6 v. By improving the membrane drawing effects the water content of the membrane increases significantly. In addition, increasing the reactant surface area enhances the capability of membrane to conduct the protons. Thus, in this model, the protonic conductivity has higher values as compared to the base model.

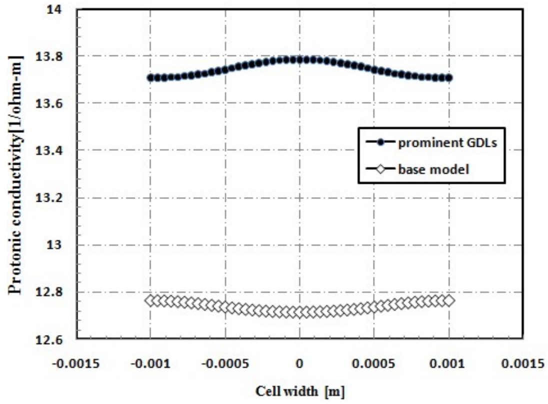

Figure 10. Comparison of the protonic conductivity in the outlet region (z=60 mm)

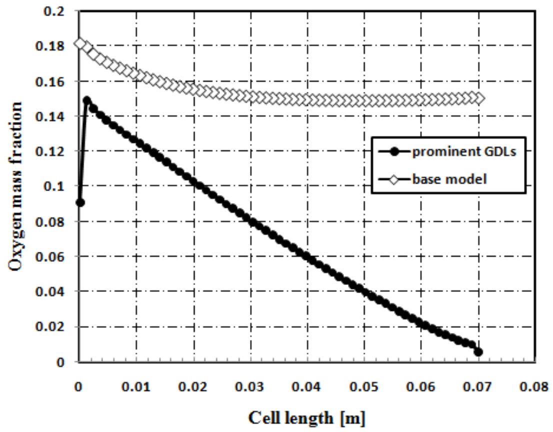

Figure 11. Comparison of oxygen mass fraction along the cell at the interface of cathode catalyst and membrane (V=0.6 v).

Figure11. illustrates the distribution of oxygen along the fuel cell for two cases under investigation. It is observed that the oxygen consumption in the case with prominences is more than the base model. The prominent case produces more current density than the base model. Therefore, the consumption of oxygen has been increased along the cell. Figures 12. and 13. justify this fact. In the prominent case the improvement in the species transferring to the reaction area leads to the enhancemen to the electrochemical reactions rates more significantly. Oxygen is consumed by moving from inlet region to the exit region, as illustrated in Figures 12. and 13. At the anode side the electrons are released by H_2 and H^+ ions are produced. The electrons pass the external circuit to reach the cathode side. This action of the electrons causes the fuel cell to generate electrical power. The protons (H^+) are shifted by water molecules toward the membrane and hereafter they reach the cathode catalyst layer surface. By the chemical reaction

between oxygen, the protons and the electrons, water molecules form at the cathode side along the cell. Therefore, the mass fraction of water increases as it is moving towards the exit regions.

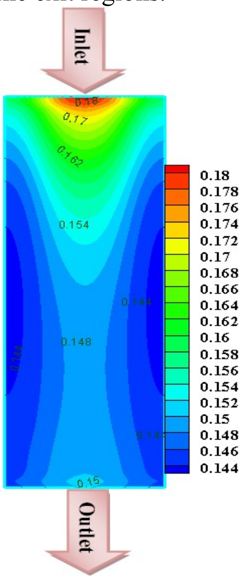

Figure 12. Oxygen mass fraction along the cell at the interface of cathode catalyst and membrane (base model)

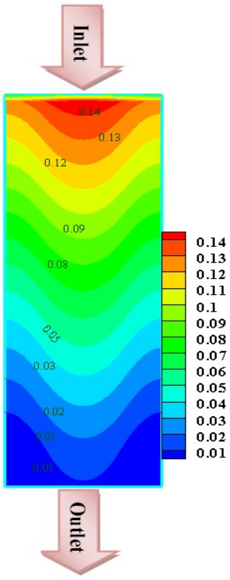

Figure 13. Oxygen mass fraction along the cell at the interface of cathode catalyst and membrane (Prominent GDLs)

Figure 14. indicates the water mass fraction at the interface of the cathode catalyst layer and the membrane. It is clearly evident that the case with prominent GDLs has more water mass fraction than the base model at the same direction. This is attributed to enhancement of the electrochemical reaction rates and improvement of water transition from the anode to the cathode side. Figures 15. and 16. illustrate the water distribution at the cathode side for the two cases studied in the present work.

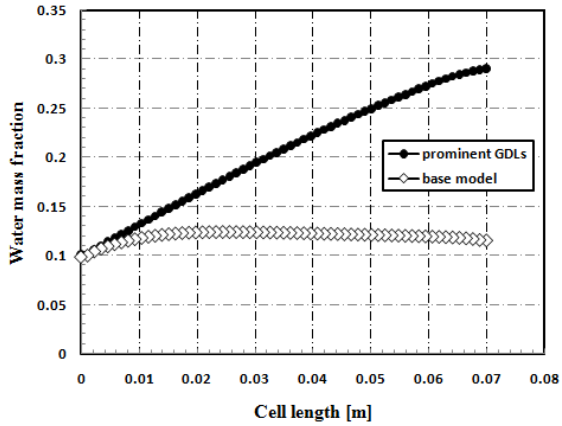

Figure 14. Comparison of water mass fraction along the cell at the interface of cathode catalyst and membrane (V=0.6 v).

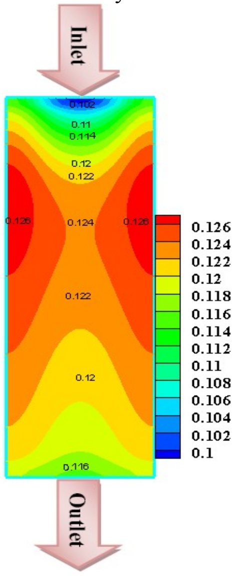

Figure 15. Water mass fraction along the cell at the interface of cathode catalyst and membrane (base model)

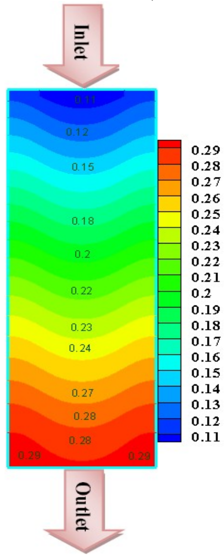

Figure 16. Water mass fraction along the cell at the interface of cathode catalyst and membrane (Prominent GDLs)

The amount of water activity depends on the water magnitude in the PEMFC. As it can be seen in Figures 14. to 16. at the cathode side the water magnitude increases. Consequently, the water activity increases at the cathode side. Figures 17. and 18. compare the water activity of the two cases studied. As expected, water activity magnitude of case with prominent GDLs is greater than that of the base model.

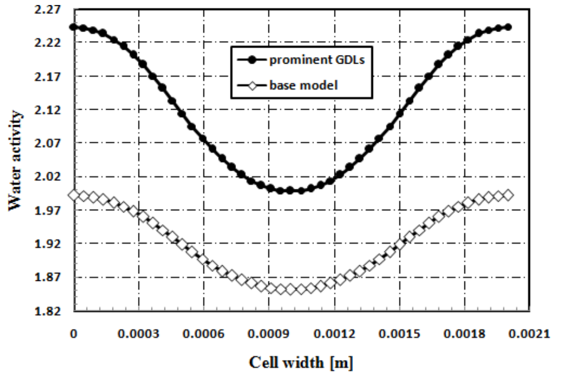

Figure 17. Comparison of water activity for two cases at inlet region (V=0.6 v)

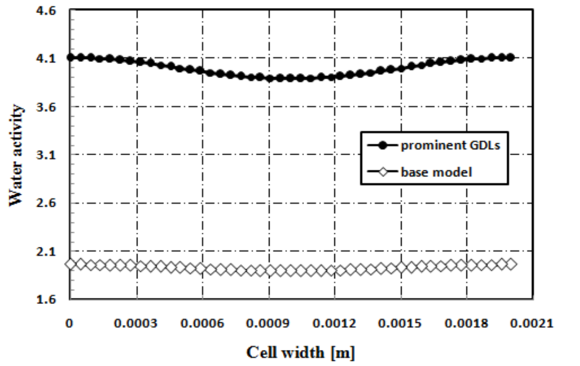

Figure 18. Comparison of water activity for two cases at outletregion (V=0.6 v).

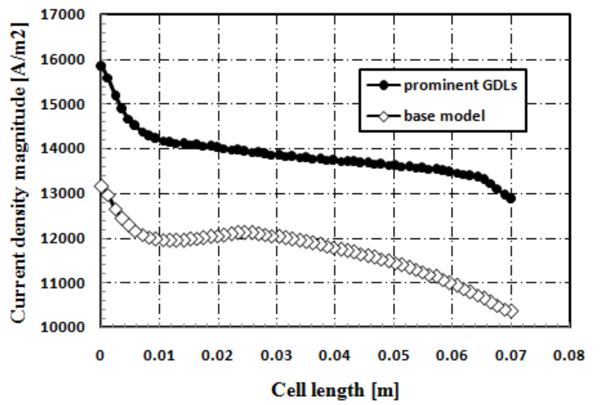

Figure 19. Comparison of the current density for the two cases at cathode catalyst.

Figure 19. compares the current density magnitude for the two cases.The produced current density decreases slightly along the cell, since the chemical reaction rate decreases due to consuming the reactant. As it can be seen, with the same operating condition, the prominent GDLs lead to more current density generation than the base model.

Figures 20. and 21. depict the temperature distribution associated with two numerical cases. The operating temperature of two models assumed to be identical (343.15 K). Electrochemical reactions takeing place at the catalyst layer leading to an increase in the cell temperature. As it is clearly evident, the prominent case has the greater value of temperatur at the same cell voltage (i.e.,0.6 V).

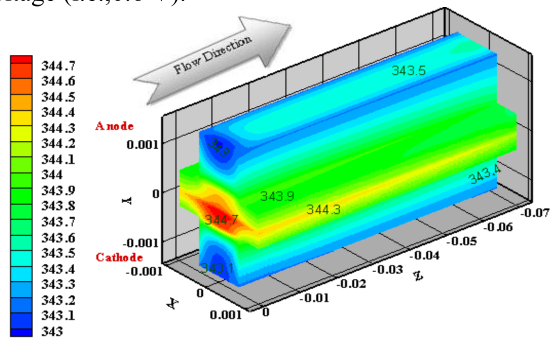

Figure 20. Temperature distribution of the base model (K)

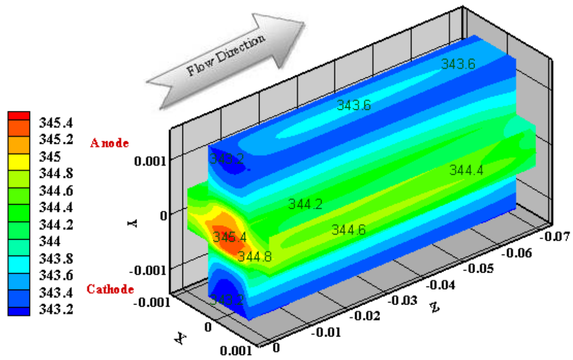

Figure 21. Temperature distribution of the case with prominent GDLs (K)

4.CONCLOUSIONS

In the present work, a three-dimensional CFD code based on the finite volume technique was developed to simulate the flow in a PEMFC having semicircular prominent GDLs. First, the accuracy of the code was substantiated through the comparison of the results associated with the base model with the available experimental data. Then the base model was developed, in order to enhance its performance, by locating semicircular prominences on the GDL layers. Polarization and power density curves, species concentration, protonic conductivity, current density magnitude diagrams and contours for both the base model and the model with semicircular prominences on GDL layers are presented and compared. The numerical results revealed that the latter model has better performance than the former model (i.e., base model) under the same operating conditions as the cell voltage, operating temperature, boundary conditions and etc. This is attributed to an increase in the diffusion surfaces area for the species in the gas channels in the latter model.The prominences reduce the cross sectional area of the channel leading to an increase in the gas velocities. Thus the convection term of the species transport increases. These factors cause the cell performance to increase.The final goal of fuel cell manufacturing is to enhance the output current density, which has been achieved in this paper.

Nomenclature

a	water activity
C	Molar concentration [mol m^{-3}]
D	Mass diffusion coeffocient [m^2 s^{-1}]
F	Faraday constant [C mol^{-1}]
I	Local current density [A m^{-2}]
J	Exchange current density [A m^{-2}]
K	Permeability [m^2]
M	Molecular mass [kg mol^{-1}]
n_d	Electro-osmotic drag coefficient
P	Pressure [Pa]
R	Universal gas constant [J mol^{-1} K^{-1}]
T	Temperature [K]
t	Thickness
u	Volocity vector
V_{cell}	Cell voltage
V_{oc}	Open-circuit voltage
W	Width
X	Mole fraction

Greek Letter

α	Water transfer coefficient
ε^{eff}	Effective porosity
ρ	Density [kg m^{-3}]
φ_e	Electrolyte phase potential (varies from -1 to 1)[v]
μ	Viscosity [kg m^{-1}s^{-1}]
σ_m	Membrane conductivity [1.ohm^{-1}m^{-1}]
λ	Water content in the membrane
ζ	Stoichiometric ratio
η	Over potential [v]
λ_{eff}	Effective thermal conductivity [w m^{-1}k^{-1}]
κ_e	Ionic conductivity
R	The transfer current
i	Local current density

Subscripts and superscripts

a	Anode
c	Cathode
ch	Channel
k	Chemical species
m	Membrane
MEA	Membrane electrolyte assembly
ref	Reference value
sat	Saturated
w	Water

5. ACKNOWLEDGMENT

This research was sponsored by Urmia University Of Technology.

REFERENCES

1. Shimpalee, S., Greenway, S. and Van Zee, J.W., "The impact of channel path length on PEMFC flow-field design", ***Journal of Power Sources,*** Vol. 160, No. 1, (2006), 398–406.
2. Yim, S.-D., Sohn, Y.-J., Yoon, Y.-G., Um, S., Kim, C.-S. and Lee, W.-Y., "Operating characteristics of 40 W-class PEMFC stacks using reformed gas under low humidifying conditions", ***Journal of Power Sources,*** Vol. 178, (2008), 711–715.
3. Perng, S.W. and Wu, H.W., "A three-dimensional numerical investigation of trapezoid baffles effect on non-isothermal reactant transport and cell net power in a PEMFC" ***Applied Energy,*** Vol. 143, (2015), 81-95.
4. Grujicic M. and Chittajallu, K.M., "Design and optimization of polymer electrolyte membrane (PEM) fuel cells", ***Applied Surface Science,*** Vol. 227, (2004), 56–72.
5. Xing, X.Q., Lum, K.W., Poh, H.J. and Wu., Y.L., "Optimization of assembly clamping pressure on performance of proton-exchange membrane fuel cells", ***Journal of Power Sources,*** Vol. 195, No. 1, (2010), 62-68.
6. Chang, W.R., Hwang, J.J., Weng, F.B. and Chan, S.H., "Effect of clamping pressure on the performance of a PEM fuel cell", ***Journal of Power Sources,*** Vol. 166, No. 1, (2007), 149-154.
7. Lange, K.J., Sui, P.C. and Djilali, N., "Determination of effective transport properties in a PEMFC catalyst layer using different reconstruction algorithms", ***Journal of Power Sources,*** Vol. 208, (2012), 354–365.
8. Amphlett, J.C., Baumert, R.M., Mann, R.F., Peppley, B.A., Roberge, P.R. and Harris, T.J., "Performance modeling of the Ballard Mark IV solid polymer electrolyte fuel cell II. Mechanistic model development", ***Journal of the Electrochemical Society,*** Vol. 142, (1995), 9-15.
9. He, G., Yamazaki, Y. and Abudula, A., "A three-dimensional analysis of the effect of anisotropic gas diffusion layer(GDL) thermal conductivity on the heat transfer and two-phase behavior in a proton exchange membrane fuel cell(PEMFC)", ***Journal of Power Sources,*** Vol. 195, No. 6, (2010), 1551–1560.
10. Kumar, N.B., Khan, A. and Chutia, J., "Composite plasma polymerized sulfonated polystyrene membrane for PEMFC." ***Materials Research Bulletin***, Vol. 70, (2015), 887-895.
11. Jinlong, L., Liang, T. and Guo, W., "Effect of strain on corrosion resistance of 316L stainless steel as bipolar plates in PEMFC environment." ***International Journal of Hydrogen Energy***, Vol. 40, No. 33, (2015), 10382–10389.
12. Uribe, F.A., Gottesfeld, S. and Zawodzinski, T.A., "Effect of ammonia as potential fuel impurity on proton exchange membrane fuel cell performance" ***Journal of the Electrochemical Society,*** Vol. 149, No. 3, (2002), A293-A296.
13. Ticianelli, E.A., Derouin, C.R. and Srinivasan, S., "Localization of platinum in low catalyst loading electrodes to attain high power densities in SPE fuel cells", ***Journal of Electroanalytical Chemistry and Interfacial Electrochemistry,*** Vol. 251, No. 2, (1988), 275–295.
14. Yao, K.Z., Karan, K., McAuley, K.B., Oosthuizen, P., Peppley, B. and Xie, T., "A review of mathematical models for hydrogen

and direct methanol polymer electrolyte membrane fuel cells", ***Fuel Cells,*** Vol. 4, (2004), 3–29.

15. Natarajan, D. and Nguyen, T.V., "A two-dimensional, two-phase, multi component, transient model for the cathode of a proton exchange membrane fuel cell using conventional gas distributors", ***Journal of the Electrochemical Society,*** Vol. 148, No. 12, (2001), A1324–A1335.
16. Ahmadi, N., Rezazadeh, S., Yekani, M.K., Fakouri, A.R. and Mirzaee, I., "Numerical investigation of the effect of inlet gases humidity on polymer exchange membrane fuel cell (PEMFC) performance", ***Transactions of the Canadian Society for Mechanical Engineering,*** Vol. 37, No. 1, (2013), 1-20.
17. Lum, K.W., McGuirk, J.J., "Three-dimensional model of a complete polymer electrolyte membrane fuel cell – model formulation, validation and parametric studies", ***Journal of Power Sources,*** Vol. 143, (2005), 103–124.
18. Ahmed, D.H. and Sung, H.J., "Effects of channel geometrical configuration and shoulder width on PEMFC performance at high current density", ***Journal of Power Sources,*** Vol. 162, (2006), 327–339.
19. Ahmadi, N., Rezazadeh, S. and Mirzaee, I., "Study the Effect of Various Operating Parameters of Proton Exchange Membrane", ***Periodica Polytechnica Chemical Engineering,*** Vol. 59, No. 3, (2015), 221-235.
20. Ahmadi, N., Pourmahmoud, N., Mirzaee, I. and Rezazadeh, S., "Three-Dimensional Computational Fluid Dynamic Study on performance of polymer exchange membrane fuel cell (PEMFC) in different cell potential***", Iranian Journal of Science and Technology,*** Vol. 36, No. 2, (2012), 129-141.
21. Ahmadi, N., Pourmahmoud, N., Mirzaee, I. and Rezazadeh, S., "Three-Dimensional Computational Fluid Dynamic Study of Effect of Different Channel and Shoulder Geometries on Cell Performance", ***Journal of Basic and Applied Sciences,*** VFol 5, No. 12, (2011), 541-556.
22. Ahmadi, N., Rezazadeh, S., Mirzaee, I. and Pourmahmoud, N., "Three-dimensional computational fluid dynamic analysis of the conventional PEM fuel cell and investigation of prominent gas diffusion layers effect", ***Journal of Mechanical Science and Technology,*** Vol. 26, No. 8, (2012), 1-11.
23. Ahmed, D.H. and Sung, H.J., "Design of a deflected membrane electrode assembly for PEMFCs", ***International Journal of Heat and Mass Transfer,*** Vol. 51, (2008), 5443–5453.
24. Kuklikovsky, A.A., "Quasi-3D Modeling of Water Transport in Polymer Electrolyte Fuel Cells", ***Journal of The Electrochemical Society,*** Vol. 150, No. 11, (2003), A1432-A1439.
25. Meredith, R.E. and Tobias, R.E., in "Advances in Electrochemistry and Electrochemical Engineering 2", (Tobias,C.W., ed., Interscience Publishers, New York, 1960).
26. Yeo S.W. and Eisenberg, A., "Physical properties and supermolecular structure of perfluorinated ion-containing (nafion) polymers", ***Journal of Applied Polymer Science,*** Vol. 21, (1977), 875-898.
27. Springer, T.E., Zawodinski, T.a. and Gottesfeld, S., "Polymer Electrolyte Fuel Cell Model", ***Journal of the Electrochemical Society,*** Vol. 136, (1991), 2334-2342.
28. Wang, L., Husar, A., Zhou, T. and Liu, H., "A parameteric study of PEM fuel cell performances", ***International Journal of Hydrogen Energy,*** Vol. 28, No. 11, (2003), 1263-1272.